Journal of Molecular Catalysis A: Chemical 407 (2015) 32–37

Contents lists available at ScienceDirect

Journal of Molecular Catalysis A: Chemical

journal homepage: www.elsevier.com/locate/molcata

Microwave-assisted hydroarylation of styrenes catalysed by transition metal oxide nanoparticles supported on mesoporous aluminosilicates

Reza Hosseinpour[a,b], Antonio Pineda[b], Angel Garcia[b], Antonio A. Romero[b], Rafael Luque[b,*]

[a] Tarbiat Modares University, Department of Organic Chemistry, Tehran, Iran
[b] Departamento de Quimica Organica, Universidad de Cordoba, Edificio Marie-Curie (C-3), Campus de Rabanales, Ctra. Nnal IV-A, Km 396, E14014, Cordoba, Spain

ARTICLE INFO

Article history:
Received 27 February 2015
Received in revised form 5 June 2015
Accepted 10 June 2015
Available online 16 June 2015

Keywords:
Supported nanoparticles
Al-SBA-15
Hydroarylation
Phenols
Styrenes

ABSTRACT

The addition of phenols to styrene to form *ortho* and *para*-(1-phenylethyl) phenols was catalysed by a range of metal oxide nanoparticles supported on mesoporous aluminosilicates (M/Al-SBA-15 catalysts) under microwave irradiation. Moderate to excellent yields to products could be obtained at short times of reaction (typically 10 min). 0.5%Fe/Al-SBA-15 as readily available, environmentally friendly and cheap catalysts exhibited remarkable improvements in yield as compared to the majority of utilized catalysts. The heterogeneous catalyst can be reused at least three times without a significant loss in activity.

1. Introduction

Alkenes are attractive starting materials for organic synthesis as they can be easily functionalized using a plethora of both oxidative and reductive mono- and difunctionalization methods [1]. In general, Friedel–Crafts alkylations and acylations are one of the most powerful methods for Carbon—Carbon bond-forming reactions [2–4]. These reactions have been traditionally performed using strong Lewis acids including $TiCl_4$, $BF_3{\cdot}OEt_2$, and $AlCl_3$ as well as mineral acids such as HF and H_2SO_4. Ongoing investigation programs are currently trying to identify and design catalysts that address typical problems in Friedel–Crafts chemistries including high catalyst loading, low selectivity, over-alkylation, formation of byproducts (salts) and sensitivity toward moisture and strong acid media.

C—H transformations of arenes and heteroarenes have recently attracted a considerable interest in organic synthesis. Protocols have been developed using various transition-metal and acid catalysts [5,6]. The addition of olefins to acetophenones [7,8] and aromatic imines [9,10], alkene additions to arenes [2,4] and heterocyclic compounds [11,12] as well as the addition of aromatics to alkynes [13,14] or alcohols [15] are elegant examples of these types of transformation. In particular, the use of aromatic-derived alkenes has been found to be very useful and practical as the resulting diarylalkane block represents an important part in biologically active compounds and pharmaceuticals substrates that include haplopappin, phenprocoumone, papaverine, or afenopin (Fig. 1).

During the past decade, transition metal nanoparticles supported on mesoporous materials emerged as promising nanoentities to develop readily available, cheaper and more efficient catalysts as alternatives to traditionally employed in several catalytic reactions, especially for their use in heterogeneous catalysis [16–18]. Nanoparticles can offer remarkably different properties as compared to bulk metals based on their degenerated density of energy states and small sizes which often lead to high activities and specificities in chemical reactions [19,20].

Solid acid catalysts are increasingly utilised in organic transformations due to their simple separation from the reaction mixture and possible reuse. Additionally, the catalytic activity of solid acid (e.g. aluminosilicates) can be increased via incorporation of metal ions such as Cu^{II}, Zn^{II}, Fe^{III}, etc., which causes the generation of highly active Lewis acid sites [21]. The combination of such active Lewis acid site along with the available Brönsted acid sites in metal-exchanged Al-SBA-15 together with the high surface area and exceptional textural properties and hydrothermal stability can facilitate reactions by localizing the reactants in

* Corresponding author.
E-mail address: q62alsor@uco.es (R. Luque).

http://dx.doi.org/10.1016/j.molcata.2015.06.010
1381-1169/

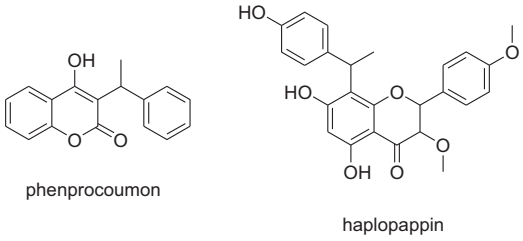

Fig. 1. Biologically and pharmaceutically active compounds.

their pores/external surfaces and providing high local concentration [22,23]. Among these transition metals, iron NPs have attracted a great interest in the design of environmentally friendly and effective catalysts as alternative to traditionally employed noble metal catalysts in several catalytic reactions. Fe-based systems have been proven to be the most effective and green system in modern organic synthesis because of their lower toxicity and easy accessibility [24,25].

In this work, we have aimed to combine the high activities and specificities of supported metal oxide nanoparticles with a simple but important C—H transformation such as the hydroarylation of styrenes with phenol derivatives [26]. A number of catalytic systems were developed and utilised in the proposed reaction under microwave irradiation.

2. Experimental

2.1. Materials synthesis

Al-SBA-15 materials were prepared in a similar way to those reported in our previous work, following the previously reported methodology by Bonardet et al. [22,27] and characterized using available techniques including X-ray diffraction (XRD), nitrogen physisorption, elemental analysis and surface acidity. Al-SBA-15 parent materials possessed a Si/Al ratio of 41 and were selected as catalyst support due to their excellent hydrothermal stabilities and textural properties (high surface area and appropriate mesoporosity) combined with a good balance of Brönsted/Lewis acid sites of moderate acidic strength. Importantly, we also needed a mechanically resistant support to the milling process utilized for the deposition of metal oxide nanoparticles.

The supported catalysts were prepared following a previously reported novel dry mechanochemical approach [28]. In a typical synthesis, 0.2 g Al-SBA-15 was ground with the needed quantity of metal precursor (e.g. $FeCl_2{\cdot}4H_2O$ or $AgNO_3$) in a Retsch PM-100 planetary ball mill using a 125 mL reaction chamber and 10 mm stainless steel balls. Milling conditions were 10 min at 350 rpm (previously optimized conditions [28]).

Upon milling, as synthesized materials were conditioned to remove the excess of unreacted and/or physisorbed precursor and directly calcined at 400 °C under air for 4 h. The conditioning step included thorough washing steps with ethanol and then acetone under mild heating (40–50 °C). Prepared catalysts, denoted as Fe0.5%AlSBA, Fe1%AlSBA, Fe2%AlSBA, Fe4%AlSBA, Ag1%AlSBA and Ag10%AlSBA, were characterized by a number of techniques including X-ray diffraction (XRD), N_2 physisorption, TEM and EDX. A similar Co10%AlSBA material was synthesized for comparative purposes.

2.2. Characterization

Structural properties of the materials were determined by XRD on a Siemens D-5000 (40 kV, 30 mA) using Cu Kα (λ = 0.15418 nm) radiation. Scans were performed over a 2θ range from 10 to 80 at step size of 0.018° with a counting time per step of 20 s.

Nitrogen adsorption measurements were carried out at 77 K using an ASAP 2000 volumetric adsorption analyzer from Micromeritics. Samples were degassed for 24 h at 130 °C under vacuum ($p < 10^{-2}$ Pa) prior to adsorption measurements. Surface areas were calculated according to the BET (Brunauer–Emmet–Teller) equation. Pore volumes (V_{BJH}) and pore size distributions (D_{BJH}) were obtained from the N_2 desorption branch.

TEM micrographs were recorded on a JEOL 2010HR instrument operating at 300 kV fitted with a multiscan CCD camera for ease and speed of use as well as with an EDX system. The lattice resolution is around 0.2 nm.

The surface acidity was measured in a dynamic mode by means of a pulse chromatographic technique of gas-phase adsorption of pyridine (PY) at 300 °C (sum of Brönsted and Lewis acid sites) and 2,6-dimethylpyridine (DMPY, Brönsted sites) as probe molecules [29].

DRIFTs characterisation of surface acidity involved the acid sites titration with PY. The basic probe was introduced by bubbling a stream of dehydrated and deoxygenated nitrogen (20 mL min^{-1}) through the liquid and into the sample chamber containing the neat (no KBr diluted) catalyst sample at 100 °C. Samples were equilibrated for at least 1 h at each temperature (100, 150, 200 or 300 °C) and reactant condition prior to collecting the spectra.

2.3. Microwave-assisted reactions

Microwave irradiation was employed as alternative energy source to promote the reactions (as opposed to conventional heating) in view of the possibilities to speed up reactions with often changes in selectivity due to the rapid and homogeneous heating achieved under microwave irradiation, particularly for supported metals [30]. In a typical reaction, 1 mmol (0.115 mL) styrene, 1.5 mmol (0.141 g) phenol, 2 mL solvent (cyclohexane) and 0.050 g catalyst were added to a pyrex vial and microwaved in a pressure-controlled CEM-Discover microwave reactor for a period of time, typically 10 min at 200 W (120 °C, maximum temperature reached) under continuous stirring. Samples were then withdrawn from the reaction mixture and analysed by GC and GC/MS Agilent 6890N fitted with a capillary column HP-5 (30 m × 0.32 mm × 0.25 μm) and a flame ionisation detector (FID).

The identity of the products was confirmed by GC–MS. Bblank reaction showed the thermal effects in the reaction were negligible (less than 5% conversion was obtained after 24 h). Response factors of the reaction products were determined with respect to the substrates from GC analysis using standard compounds in calibration mixtures of specified compositions. The microwave method was generally power controlled (by an infra-red probe) where the samples were irradiated with the required power output (settings at maximum power, 300 W) to achieve different temperatures in the range of 115–120 °C.

3. Results and discussion

Textural and surface properties of the materials have been summarized in Table 1. Surface acidities measured using pyridine (PY) and 2,6-dimethylpyridine (DMPY) as probe molecules pointed to a significant increase of Lewis acidity (difference between PY-DMPY values) upon Fe incorporation in the materials. These findings are in good agreement with previous reports from the group [23,28]. In any case, ball-milling (BM) synthesized nanomaterials possessed similar textural properties (e.g. surface areas, pore size and volumes) as compared to the parent aluminosilicate. Comparatively, the incorporation of Ag into the SBA-15 aluminosilicate material

Table 1
Textural properties [surface area ($m^2\ g^{-1}$), pore size (nm) and pore volume ($mL\ g^{-1}$)] and surface acidity [measured as mmol adsorbed of probe molecule (PY or DMPY) per gram of catalyst] of metal NPs supported on mesoporous materials and parent Al-SBA-15.

				Surface acidity at 300 °C (μmol base g^{-1})	
Catalyst	Metal loading (wt%)	Surface area ($m^2\ g^{-1}$)	Pore size/volume (nm/$mL\ g^{-1}$)	PY (total acidity)	DMPY (Brönsted acidity)
Al-SBA-15	–	762	6.4/ 0.60	81	77
Fe0.5/AlSBA	0.9	630	6.3/0.48	150	90
Fe1/AlSBA	1.1	663	6.3/0.61	111	96
Fe2/AlSBA	2.3	645	6.3/0.50	141	87
Fe4/AlSBA	4.0	655	6.8/0.52	110	90
Ag1/AlSBA	0.7	512	6.5/0.46	126	116
Ag10/AlSBA	11.7	606	6.7/0.57	108	97
Co10/AlSBA	9.6	492	6.0/0.33	144	100

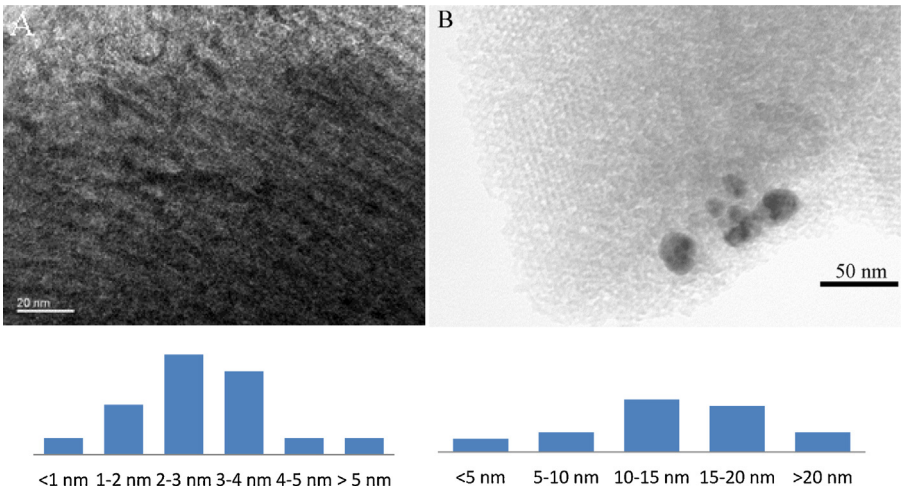

Fig. 2. TEM images of Fe0.5/AlSBA (left) and Ag10/AlSBA (right) with their corresponding size distribution histograms underneath. An average of ca. 20 nanoparticles were size-measured for the preparation of the histograms.

equally increased both Lewis and Bronsted acidities (particularly for the 1%Ag material). Metal loadings determined by ICP/MS were generally close to theoretical values in most cases, except for the case of Fe0.5%/AlSBA in which a larger Fe content was observed (Table 1). Supported nanoparticle systems exhibited reduced surface areas but in general fairly similar related textural properties (pore sizes and volumes) as compared to the parent Al-SBA-15. XPS characterization of mechanochemically synthesized nanomaterials indicated the presence of metal oxides (Fe_2O_3, hematite phase [23,28] and AgO) as indicated by the typical binding energies (711.7 eV for Fe $2p_{3/2}$ and 367.5 eV for Ag 3d 5/2) characteristic of previously reported similar metal oxide Fe_2O_3 [31,32] and AgO species [33,34]. Nanomaterials were further characterized by TEM microscopy which confirmed the presence of nanoparticles supported on the mesoporous aluminosilicates (Figs. 2 and 3). Fe-containing Al-SBA materials possessed relatively small nanoparticles in size (typically between 2-7 nm depending on the material, see Figs. 2 A and 3) as compared to larger AgO nanoparticles observed for Ag1 and particularly higher loaded Ag10/AlSBA (ca. 14 nm average nanoparticle size, Fig. 2B).

Initially, a preliminary solvent screening was conducted in order to find out the optimum solvent conditions for the reaction.

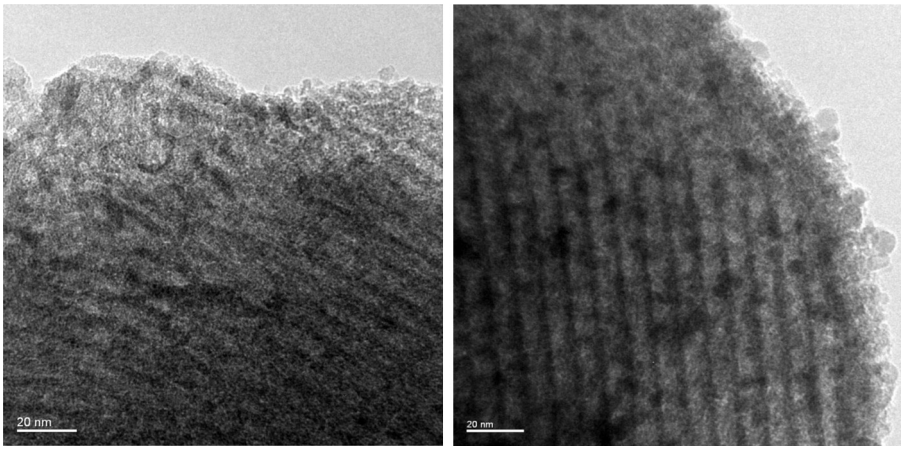

Fig. 3. Representative TEM images of Fe0.5/AlSBA (left) and Fe4/AlSBA (right). A significant differences in nanoparticle size can be observed between materials. Nanoparticles can be clearly visualized as dark spots in TEM images.

Table 2
Solvent screening in the hydroarylation of styrene with phenol using Fe0.5%/AlSBA.[a]

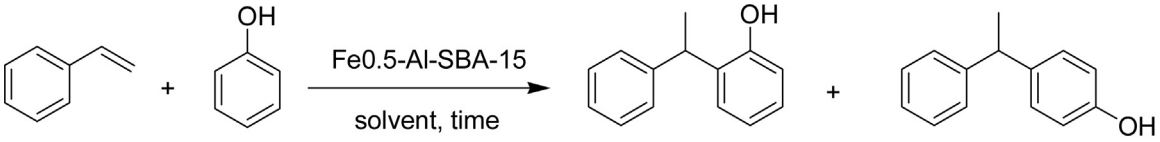

ortho-(1-phenylethyl)phenol *para*-(1-phenylethyl)phenol

Entry	Solvent	Conversion (%)[b]	Selectivity (*ortho*-:*para*-)[c]
1	ACN	–	–
2	DMF	–	–
3	Toluene	70	61:38
4	Ethyl acetate	–	–
5	Ethanol	–	–
6	DCM	94	60:39
7	Cyclohexane	>99	56:43

[a] Reaction conditions: (1 mmol, 0.115 mL) styrene, (1.5 mmol, 0.141 g) phenol, 0.050 g catalyst, 2 mL solvent, 200 W, 10 min reaction, T = 120 °C.
[b] GC conversion of styrene.
[c] GC yield of arylated products.

Fe0.5%/Al-SBA-15 was selected as catalyst for solvent optimisation based on previous results of the group which pointed out the optimum activities of Fe0.5%/Al-SBA-15 with respect to other catalytic systems in C—H transformations [35]. Results summarized in Table 2 indicated that cyclohexane is the solvent of choice (Table 2, entry 7). Although the reaction did not proceed in acetonitrile, DMF, ethylacetate and ethanol after 10 min, almost quantitative conversion of styrene was observed in dichloromethane (DCM), with a good conversion also in toluene. Comparatively, complete conversion of styrene to products was observed in cyclohexane within a remarkable short reaction time (Table 2, entry 7). These findings were in good agreement with previously reported literature results [23,35].

Different nanomaterials were subsequently investigated under typically short reaction times (10 min) in the same microwave-assisted model reaction in cyclohexane. Upon reaction optimisation, Table 3 summarises the main findings of this work. Blank runs (in the absence of catalyst) provided no conversion in the systems (entry 1), while the acidic Al-SBA-15 support gave an interesting 64% conversion after 10 min of reaction with an improved selectivity to the *para*- isomer (entry 2). As compared to various M-Al-SBA-15, the corresponding Fe0.5/AlSBA exhibited optimum activities in the reaction at times of reaction of 10 min (Table 3, entry 3). *Ortho*-(1-phenylethyl) phenol (55%) was obtained as favoured reaction product. Ag1/AlSBA also provided quantitative conversion in the systems, with a 60% selectivity to the *para*- derivative (Table 3, entry 7).

Importantly, the effect of metal loading in the catalytic activity was investigated in both Fe and Ag-containing materials. An increase in metal loading (from 0.5 to 4 wt.%) in Fe/Al-SBA-15 materials involved a gradual decrease in conversion as well as an interesting switch in selectivity from *ortho*- to *para*- (Table 3, entries 3 to 6). A similar effect was observed when comparing the activity of Ag1 and Ag10/AlSBA materials (Table 3, entries 7 and 8) as well as a Co10/AlSBA. These findings in fact pointed out that the catalytic activity in the systems is not only influenced by acidity (i.e. Fe0.5 and Fe2/AlSBA have almost identical textural and surface acid properties, see Table 1) but most importantly nano-effects including nanoparticle size and dispersion could be playing a major role in the observed differences. TEM analysis was subsequently conducted in this regard and a comparison between two Fe-containing materials (Fe0.5 and Fe4/AlSBA) has been included in Fig. 3.

TEM images evidenced significant differences in terms of nanoparticle sizes for Fe0.5 (2.5 nm, average particle size) and Fe4/AlSBA (7 nm, average particle size) which can be correlated with the significantly different catalytic activities in both materials. In general, nanoparticle sizes were found to gradually increase with metal loading. These results were also in good agreement with reduced catalytic activities found for high loaded Ag and Co-containing materials (e.g. Ag10/AlSBA and Co10/AlSBA, Table 2) despite their relatively similar textural and surface acid properties as compared to low-loaded highly active materials (Table 1).

The recycling and stability of the catalyst under the investigated conditions was subsequently studied (Fig. 4). After each cycle, the reaction mixture was allowed to cool down to room temperature and the catalyst was separated by filtration. The recov-

Table 3
Effect of catalyst and time in the hydroarylation of phenol with styrene.[a]

Entry	Catalyst	Conversion (%)[b]	Selectivity (*ortho*-/ *para*-[c])
1	Blank	–	–
2	Al-SBA-15	64	45:55
3	Fe0.5/AlSBA	>99	56:44
4	Fe1/AlSBA	88	45:55
5	Fe2/AlSBA	85	39:61
6	Fe4/AlSBA	63	47:53
7	Ag1/AlSBA	>99	40:60
8	Ag10/AlSBA	<15	88:12
9	Co10/AlSBA	74	55:45

[a] Reaction conditions: (1 mmol, 0.115 mL) of styrene, (1.5 mmol, 0.141 g) of phenol, 50 mg of catalyst, 2 mL of cyclohexane, 200 W, 10 min reaction, T = 115 – 120 °C.
[b] GC conversion of styrene.
[c] GC yield of arylated products.

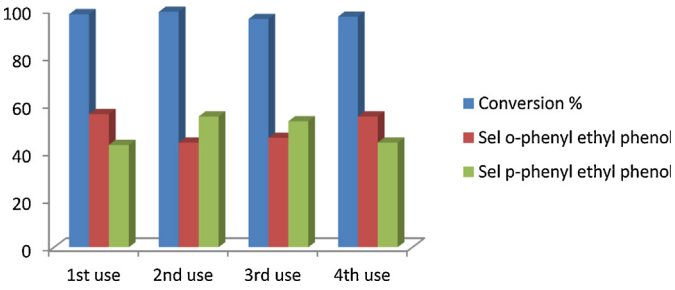

Fig. 4. Reusability studies of Fe0.5/AlSBA in the Reaction of Phenol with Styrene. Reaction conditions: 1 mmol (0.115 mL) styrene, 1.5 mmol (0.141 g) phenol, 50 mg of catalyst, 2 mL of cyclohexane, 200 W, T = 120 °C, 10 min reaction per run.

Table 4
Scope of the hydroarylation reaction using phenol derivatives and styrene.[a]

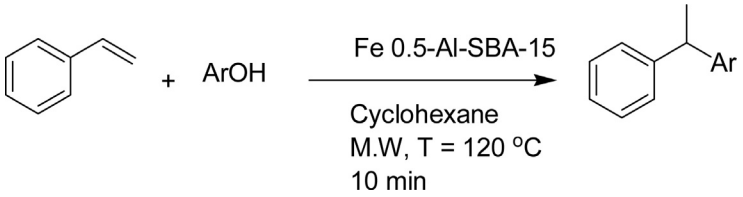

Entry	ArOH	Time (min)	Conversion (mol%)[b]	Selectivities (mol%)[c]
1	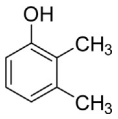	10	81	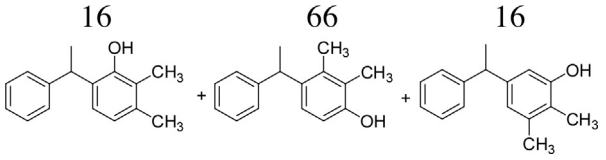 16 66 16
2	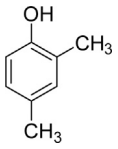	10	<20	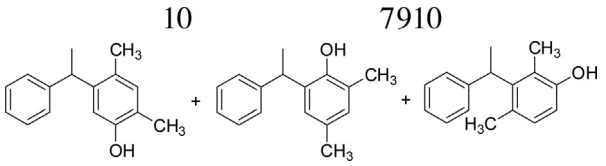 10 7910
3	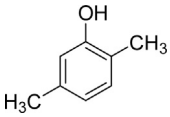	10	90	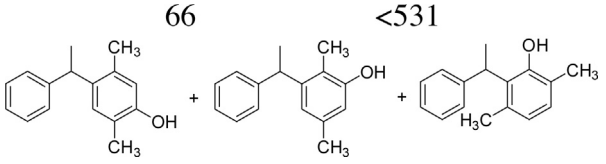 66 <531
4	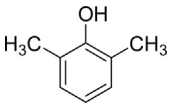	10	>99	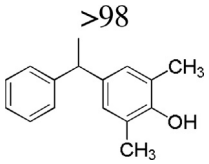 >98
5	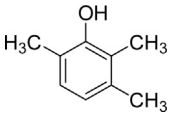	10	82	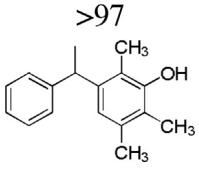 >97
6	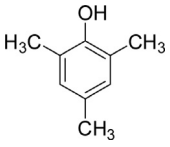	10	96	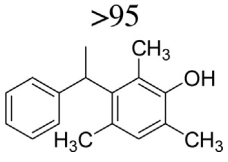 >95

[a] Reaction conditions: (1 mmol, 0.115 mL) styrene, (1.5 mmol) phenol derivatives, 0.05 g Fe0.5/AlSBA, 2 mL of solvent, 200 W, $T = 120\,^{\circ}C$.
[b] GC conversion of styrene.
[c] GC yield of isomers.

ered catalyst was then washed with cyclohexane, methanol and dichloromethane and dried at 100 °C for 4 h. The catalyst was then reused without any further treatment. The recycled Fe0.5/AlSBA catalyst exhibited an excellent conversion under the investigated reaction conditions, preserving over 90% of their initial activity after four uses.

To explore the scope and limitation of the reaction, the optimized conditions were subsequently extended to several other substituted phenols (Table 4). Different isomers could be obtained depending on the substituent and directing groups on the phenol ring. In any case, excellent styrene conversion to target products could be achieved in most cases after 10 min of reaction, with the exception of 2,4-dimethylphenol (Table 4, entry 2).

4. Conclusions

A simple and efficient protocol has been developed for the hydroarylation of phenols with styrene catalysed by supported nanoparticles on mesoporous Al-SBA-15 under microwave irradiation. Fe0.5/AlSBA provided optimised yields to products under mild reaction conditions and short times of reaction (typically 10 min). Catalysts were highly stable and reusable under the investigated conditions up to four uses, with a protocol also amenable to a range of substituted phenols. The designed supported nanoparticle systems are envisaged to have a remarkable potential for further coupling and oxidation chemistries that will be reported in due course.

Acknowledgments

Rafael Luque gratefully acknowledges Spanish MICINN for financial support via the concession of a RyC contract (ref: RYC-2009-04199) and funding under project CTQ2011-28954-C02-02 (MEC). Consejeria de Ciencia e Innovacion, Junta de Andalucia is also gratefully acknowledged for funding project P10-FQM-6711.

References

[1] M. Beller, J. Seayad, A. Tillack, H. Jiao, Angew. Chem. Int. Ed. 43 (2004) 3368.
[2] M. Bandini, A. Melloni, A.U. Ronchi, Angew. Chem. Int. Ed. 43 (2004) 550.
[3] G. Olah, V. Prakash Reddy, G.K. Surya Prakash, Kirk-Othmer Encyclopedia of Chemical Technology, Hoboken, 2000.
[4] G.K. Surya Prakash, P.J. Linarez-Palomino, K. Glinton, S. Chacko, G. Rasul, T. Mathew, G.A. Olah, Synlett 7 (2007) 1158.
[5] F. Muhlthau, O. Schuster, T. Bach, J. Am. Chem. Soc. 127 (2005) 9348.
[6] J. Liu, E. Muth, U. Flörke, G. Henkel, K. Merz, J. Sauvageau, E. Schwalke, G. Dyker, Adv. Synth. Catal. 348 (2006) 456.
[7] F. Kakiuchi, T. Uetsuhara, Y. Tanaka, N. Chatani, S. Murai, J. Mol. Catal. A: Chem. 182 (2002) 511.
[8] Y. Guari, A. Castellanos, S. Sabo-Etienne, B. Chaudret, J. Mol. Catal. A: Chem. 212 (2004) 77.
[9] F. Kakiuchi, M. Yamauchi, N. Chatani, S. Murai, Chem. Lett. (1996) 11.
[10] C.-H. Jun, J.-B. Hong, Y.-H. Kim, K.-Y. Chung, Angew. Chem. Int. Ed. 39 (2000) 3440.
[11] R.K. Thalji, K.A. Ahrendt, R.G. Bergman, J.A. Ellman, J. Am. Chem. Soc. 123 (2001) 9692.
[12] K.A. Ahrendt, R.G. Bergman, J.A. Ellman, Org. Lett. 5 (2003) 1301.
[13] F. Kakiuchi, Y. Yamamoto, N. Chatani, S. Murai, Chem. Lett. (1995) 681.
[14] C.G. Jia, W.T. Lu, J. Oyamada, T. Kitamura, K. Matsuda, M. Irie, Y. Fujiwara, J. Am. Chem. Soc. 122 (2000) 7252.
[15] J. Choudhury, S. Podder, S. Roy, J. Am. Chem. Soc. 127 (2005) 6162.
[16] A.P. Wight, M.E. Davis, Chem. Rev. 102 (2002) 3589.
[17] A. Corma, H. Garcia, Chem. Rev. 102 (2002) 3837.
[18] T. Mallat, A. Baiker, Chem. Rev. 104 (2004) 3037.
[19] R.J. White, R. Luque, V. Budarin, J.H. Clark, D.J. Macquarrie, Chem. Soc. Rev. 38 (2009) 481.
[20] J.M. Campelo, D. Luna, R. Luque, J.M. Marinas, A.A. Romero, ChemSusChem 2 (2009) 18.
[21] Z. Luan, M. Hartmann, D. Zhao, W. Zhou, L. Kevan, Chem. Mater. 11 (1999) 1621.
[22] C. Gonzalez-Arellano, R.A.D. Arancon, R. Luque, Green Chem. 16 (2014) 4985.
[23] A.M. Balu, A. Pineda, K. Yoshida, J.M. Campelo, P.L. Gai, R. Luque, A.A. Romero, Chem. Commun. 46 (2010) 7825.
[24] T. Stemmler, A.E. Surkus, M.M. Pohl, K. Junge, M. Beller, ChemSusChem 7 (2014) 3012.
[25] Iron Catalysis: Fundamentals and Applications, in: B. Plietker (Ed.), Springer, The Netherlands, 2011.
[26] S. Haldar, S. Koner, J. Org. Chem. 75 (2010) 6005.
[27] B. Jarry, F. Launay, J.P. Nogier, V. Montouillout, L. Gengembre, J.L. Bonardet, Appl. Catal. A: Gen. 309 (2006) 177.
[28] A. Pineda, A.M. Balu, J.M. Campelo, A.A. Romero, D. Carmona, F. Balas, J. Santamaria, R. Luque, ChemSusChem 41 (2011) 561.
[29] J.M. Campelo, D. Luna, R. Luque, J.M. Marinas, A.A. Romero, J.J. Calvino, M.P. Rodríguez-Luque, J. Catal. 230 (2005) 327.
[30] C.O. Kappe, B. Pieber, D. Dallinger, Angew. Chem. Int. Ed. 52 (2013) 1088–1094.
[31] Handbook of X-Ray Photoelectron Spectroscopy, in: C.D. Wagner, W.N.L.E. Riggs, G.F. Davis, G.E. Moulder (Eds.), Muilenberg, Perkin Elmer, Eden Prairie, 1979.
[32] X. Deng, J. Lee, D. Matranga, Surf. Sci. 604 (2010) 627.
[33] <http://www.xpsfitting.com/2013/04/silver.html/>.
[34] G.B. Hoflund, Z.F. Hazos, G.N. Salaita, Phys. Rev. B 62 (2000) 11126.
[35] R. Hosseinpour, A. Pineda, A. Garcia, A.A. Romero, R. Luque, Catal. Commun. 48 (2014) 73.